

Thermal fading of the $1/k^4$ -tail of the momentum distribution induced by the hole anomaly

Giulia De Rosi,^{1,*} Grigori E. Astrakharchik,^{1,2,†} Maxim Olshanii,³ and Jordi Boronat^{1,‡}

¹Departament de Física, Universitat Politècnica de Catalunya, Campus Nord B4-B5, 08034 Barcelona, Spain

²Departament de Física Quàntica i Astrofísica, Facultat de Física, Universitat de Barcelona, E-08028 Barcelona, Spain

³Department of Physics, University of Massachusetts Boston, Boston Massachusetts 02125, USA

(Dated: February 13, 2023)

We provide the ab-initio Path Integral Monte Carlo calculation of the momentum distribution in a one-dimensional repulsive Bose gas at finite temperatures. We explore all interaction and thermal regimes. An important reference temperature is that of the hole anomaly, observed as a peak in the specific heat and a maximum in the chemical potential. We find that at large momentum k and temperature above the anomaly threshold, the universal tail \mathcal{C}/k^4 of the distribution (proportional to the Tan's contact \mathcal{C}) is screened by the $1/|k|^3$ -term due to a dramatic thermal increase of the internal energy. The same fading is consistently revealed in the short-distance behavior of the one-body density matrix (OBDM) where the $|x|^3$ -dependence disappears for temperatures above the anomaly. At very high temperatures, the OBDM and the momentum distribution approach the Gaussian of classical gases. We obtain a new and general analytic tail for the momentum distribution and a minimum k fixing its range of validity, both calculated with Bethe-Ansatz and valid for any interaction strength and temperature.

Ultracold atomic gases are versatile tools to study quantum phenomena with unprecedented controllability and purity. The Bardeen-Cooper-Schrieffer (BCS) theory [1–3], originally developed to explain conventional superconductivity in solid-state materials, was confirmed even by the Cooper pairing in interacting Fermi gases [4]. Bose-Einstein condensate (BEC) manifests macroscopic quantum behavior, superfluidity, and coherence and was neatly realized in Bose gases after 70 years since its prediction [5–7].

Tan's contact \mathcal{C} is defined in any system where interactions can be approximated by a s -wave potential with zero range (universal regime) [8], which is well justified in ultracold gases due to their extreme diluteness [9–12]. \mathcal{C} provides a fundamental connection between macroscopic thermodynamic quantities (internal energy) and microscopic large-momenta (short-distance) correlations.

\mathcal{C} gives the strength of the tail of the momentum distribution $n(k)$ at high momenta k through the universal law $n(k) \sim \mathcal{C}/k^4$ [10–12] which is valid for any quantum system and any spatial dimension, and is independent of its quantum statistics. This law applies to nucleons [13] and ultracold atoms [9, 14]. $n(k) \sim 1/k^4$ was related to the interaction dependence of the internal energy in a one-dimensional repulsive Bose gas at zero temperature [9]. Later, S. Tan defined the contact and derived the same result in the BCS-BEC crossover of three-dimensional fermionic ensembles at arbitrary temperature [11, 12]. Theoretically, this universal law is considered valid for multicomponent systems of both quantum statistics [15, 16] and below and above the critical temperature T_c of the superfluid phase transition [8, 17]. $n(k) \sim \mathcal{C}/k^4$ has been experimentally confirmed in Fermi atomic gases only at low temperature [18], but not in the Bose counterpart raising the question if exists a temperature above which it is violated [19].

One-dimensional (1D) systems are appealing as the interaction can be strong without compromising stability. They exhibit an *Anomaly*, i.e. a thermal feature in the thermodynamic quantities as a function of temperature, identified by a peak in the specific heat, a maximum in the chemical potential or

a minimum in the magnetization, located at the anomaly temperature T_A . It signals the presence of unpopulated states in the excitation spectrum of Bose/Fermi ensembles [20], spin chains [21, 22] and ladders [23, 24]. When the temperature T is comparable to T_A , states are thermally occupied and the internal energy rapidly increases with temperature at $T > T_A$.

In a 1D contact repulsive Bose gas, the *Hole Anomaly* has been recently predicted for any interaction strength [20]. Path Integral Monte Carlo (PIMC) results for the dynamic structure factor showed that, at $T \sim T_A$, the excitations experience the breakdown of the low- T quasiparticle description which is replaced by thermal fluctuations at $T > T_A$ [20]. This anomaly is a reminiscence of a superfluid transition occurring at T_c in higher dimensions, although phase transitions are forbidden in 1D [25]. In a 1D Bose gas at $T < T_A$, $n(k) \sim \mathcal{C}/k^4$ agrees with PIMC results at large k [26]. No knowledge at $T > T_A$ was available so far and an open question is how the tail of $n(k)$ changes across the anomaly.

We report that the thermal increase of the internal energy, induced by the hole anomaly, is responsible for the suppression of the tail $n(k) \sim \mathcal{C}/k^4$ at $T > T_A$. The $1/|k|^3$ -term becomes dominant as depends on the internal energy. This thermal fading occurs for any interaction as shown by comparison with PIMC results. It may be observed in 1D atomic Bose gases where $n(k)$ has been measured [27–30] and the exploration of a wide range of interaction strength and temperature, below and above the anomaly, is possible [31].

Model.— We consider a 1D uniform gas composed of N repulsive Bose particles interacting via contact-pairwise potential and described by the Hamiltonian:

$$H = -\frac{\hbar^2}{2m} \sum_{i=1}^N \frac{\partial^2}{\partial x_i^2} + g \sum_{i>j}^N \delta(x_i - x_j), \quad (1)$$

where m is the particle mass, $g = -2\hbar^2/(ma) > 0$ is the 1D coupling constant [32], and $a < 0$ is the 1D s -wave scattering length. We study the thermodynamic limit by increasing the system size $L \rightarrow \infty$ while keeping the linear density $n =$

N/L fixed. The interaction strength is $\gamma = -2/(na)$.

There are no phase transitions but rather a continuous crossover that encompasses different quantum degeneracy regimes in terms of γ and temperature. At zero temperature $T = 0$, the gas admits a mean-field description [8] in the Gross-Pitaevskii (GP) limit of weak repulsion $\gamma \ll 1$, which in 1D corresponds to high density $n|a| \gg 1$. In the Tonks-Girardeau (TG) regime of strong repulsion $\gamma \gg 1$, achieved at low density $n|a| \ll 1$, bosons become impenetrable and the wavefunction is mapped [33] onto that of an ideal Fermi gas, resulting in identical thermodynamics and spectrum. Many experiments explored the GP-TG crossover in ultracold atom platforms [34–40]. At $T = 0$, the energetic properties of the Lieb-Liniger model can be obtained using the Bethe-Ansatz method [8, 41–43]: the ground-state energy E_0 , chemical potential $\mu_0 = (\partial E_0 / \partial N)_{a,L}$ and speed of sound $v = \sqrt{n/m(\partial \mu_0 / \partial n)_a}$ which are all functions of γ .

At finite temperature T , the thermal Bethe Ansatz (TBA) [44, 45] can be used and the thermodynamics within the canonical ensemble is captured by the Helmholtz free energy $A = E - TS$, where E is the internal energy and S the entropy. The Tan's contact is [46–48]

$$\mathcal{C} = (4m/\hbar^2) (\partial A / \partial a)_{T,N,L}, \quad (2)$$

which also provides information on the interaction energy and a relation between pressure and E [9–12, 14, 48, 49].

In Fig. 1, we report the exact thermal Bethe-Ansatz results of the internal energy per particle E/N as a function of temperature and for characteristic values of the interaction strength γ . We show energies in units of the Fermi value $E_F = k_B T_F = \hbar^2 \pi^2 n^2 / (2m)$ and temperatures rescaled by the quantum degeneracy threshold $T_d = T_F / \pi^2$. Vertical lines denote the hole-anomaly temperature T_A for each value of γ , estimated from the peak in the specific heat [20]. For any γ , E is almost constant for $T \lesssim T_A$, while it exhibits an intense monotonic increase at higher temperatures $T > T_A$.

One-Body Density Matrix.— The one-body density matrix (OBDM) is defined by the non-diagonal number [8]:

$$g_1(x = x_1 - x_2) = \langle \hat{\psi}^\dagger(x_1) \hat{\psi}(x_2) \rangle, \quad (3)$$

where $\hat{\psi}(x)$ is the Bose field, x the interparticle distance and $\langle \dots \rangle$ denotes the average over an ensemble in thermal equilibrium at T . The OBDM quantifies the coherence and corresponds to the amplitude of the process where one particle is annihilated at position x_2 and the state is recovered by creating a particle at x_1 . At $x = 0$, one finds the density n . The momentum distribution is the Fourier transform of the OBDM.

We used PIMC to calculate the complete x -dependence of the OBDM for a wide range of interaction strength γ and temperature in a 1D Bose gas [49]. At high temperatures, $T \gg T_d$, PIMC results show an excellent agreement with the Maxwell-Boltzmann (MB) Gaussian law $g_1(x)_{\text{MB}} = ne^{-x^2/(2\sigma^2)}$ [49] describing a classical gas and decaying to zero for $x \gg \sigma$ where $\sigma = \lambda/\sqrt{2\pi}$ is the standard deviation proportional to the thermal wavelength $\lambda = \sqrt{2\pi\hbar^2/mk_B T}$.

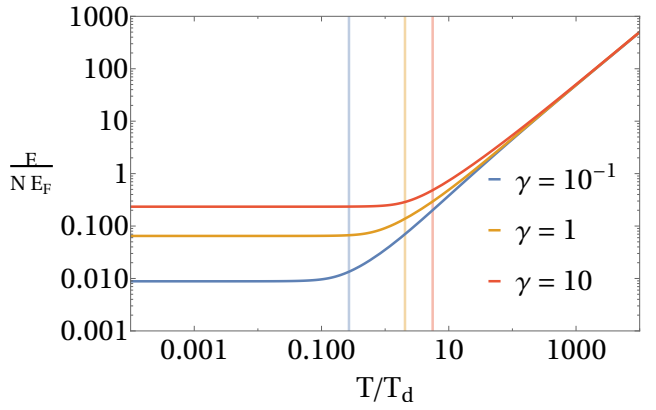


Figure 1. Internal energy per particle E/N normalized to the Fermi value $E_F = k_B T_F = \hbar^2 \pi^2 n^2 / (2m)$ vs temperature in units of the quantum degeneracy threshold $T_d = T_F / \pi^2$ and for several interaction strengths γ reported from small (bottom) to large (top) values. Calculations have been performed with TBA. Vertical lines denote the anomaly temperature T_A/T_d from small (left) to large (right) γ , corresponding to 0.27 ($\gamma = 10^{-1}$), 2.05 ($\gamma = 1$) and 5.58 ($\gamma = 10$).

The short-distance expansion of the OBDM is [50]

$$\frac{g_1(|x| \lesssim x_{\max})}{n} = 1 + \sum_{i=1}^{\infty} c_i (xn)^i + b_3 |xn|^3 + \mathcal{O}(|xn|^4). \quad (4)$$

The coefficients c_i in the Taylor expansion of the analytic part are the corresponding moments of the momentum distribution [50], they diverge for $i > 3$ and the odd ones vanish $c_1 = c_3 = \dots = 0$. From the Hellmann-Feynman theorem [51], one finds that the second coefficient is a function of the internal energy E/N and Tan's contact \mathcal{C}/N per particle:

$$c_2 = -\frac{1}{2} \left(\frac{E}{N} \frac{2m}{\hbar^2 n^2} - \frac{\mathcal{C}}{N} \frac{1}{\gamma n^3} \right), \quad (5)$$

and c_2 can be also expressed in terms of the average kinetic energy [8, 49]. The non-analytic part of Eq. (4) starts with a $|x|^3$ dependence whose coefficient depends on \mathcal{C}/N only:

$$b_3 = (\mathcal{C}/N) / (12n^3). \quad (6)$$

Equations (4–6) have been derived at $T = 0$ [9]. The finite- T dependence enters in E and \mathcal{C} which can be evaluated exactly with TBA [44, 45, 48, 49]. Eq. (4) is valid for any value of γ and T as shown by comparison with PIMC calculations [49].

We find that Eq. (4) holds up to a maximal distance

$$x_{\max} = (\xi^{-1} + \sigma^{-1})^{-1} \quad (7)$$

and is determined by the healing length $\xi = \hbar/(\sqrt{2}mv)$ and the standard deviation σ of the Gaussian $g_1(x)_{\text{MB}}$. At $T = 0$, the empirical expression (7) reduces to $x_{\max} = \xi$ which constrains the high-momentum range for the tail of the momentum distribution $n(|k| \gtrsim \xi^{-1})$ [52]. At high temperatures, we recover instead the classical gas limit $x_{\max} = \sigma$.

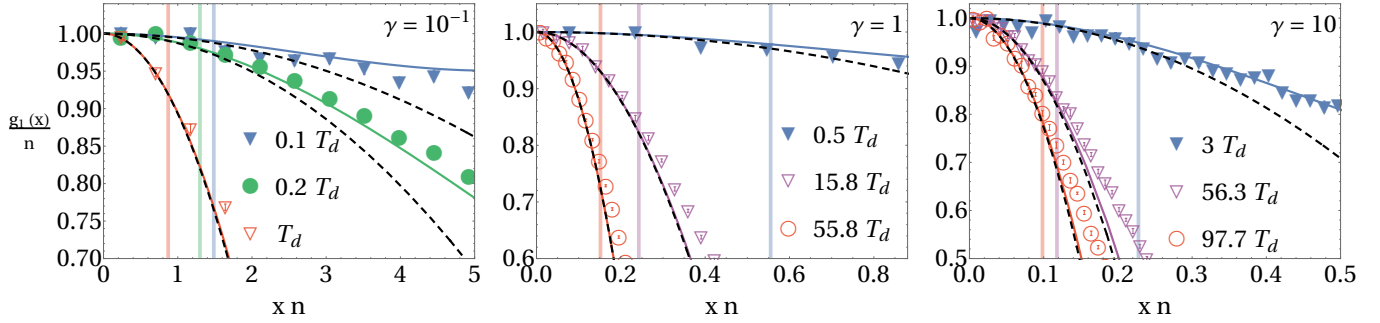


Figure 2. OBDM $g_1(x)/n$ vs mean inter-particle distance xn for $\gamma = 10^{-1}$ (first panel), $\gamma = 1$ (second), and $\gamma = 10$ (last) and different temperatures. Symbols denote PIMC results and their sizes are larger than the error bars. Solid (empty) symbols correspond to temperatures below (above) the anomaly value T_A , Fig. 1. Solid lines represent the short-distance expansion (4) calculated with TBA. Dashed black lines correspond to Eq. (4), but with $b_3 = 0$. Curves are reported in increasing order of the temperature from low (top) to high (bottom) values. Maximal distance of the expansion $x_{\max}n$ (7) is shown with vertical lines with increasing T from low (right) to high (left).

In Fig. 2, we show exact PIMC results of the one-body density matrix. Solid symbols correspond to temperatures below the hole anomaly $T < T_A$, while empty ones for $T > T_A$. Weakly- ($\gamma = 10^{-1}$, first panel), intermediate- ($\gamma = 1$, second) and strongly- ($\gamma = 10$, last) interacting regimes are reported. We test the importance of the non-analytic contribution by comparing the short-distance OBDM, Eq. (4), with $b_3 \neq 0$ (colored solid lines) and $b_3 = 0$ (black dashed), calculated with TBA. x_{\max} (7) is shown with vertical lines.

Our results are valid for any interaction strength γ and can be summarized as: (i) the short-range expansion (4) of the OBDM holds at distances limited by Eq. (7) at any temperature, as witnessed by the comparison of Eq. (4) with PIMC; (ii) the non-analytic term (with coefficient b_3) in Eq. (4) is indispensable for an accurate description at $T < T_A$, while it can be safely neglected at $T > T_A$. The physical reason is that the internal energy increases rapidly at $T > T_A$, see Fig. 1, making b_3 (6) small compared to the c_2 coefficient (5). Thus, the thermal fading of the $|x|^3$ -dependence in the short-distance OBDM is driven by the hole anomaly.

In the high-temperature MB regime [53], we obtain: $x_{\max} = \sigma$; $E/N = k_B T/2$ as the energy is defined by thermal fluctuations [20] and contact $\mathcal{C} = 0$ as interactions are negligible, Eq. (2). The short-range behavior (4) of the OBDM is described by analytic terms coming from the expansion of the Gaussian $g_1(x \lesssim \sigma)_{\text{MB}}/n = 1 - (x/\sigma)^2/2 + \mathcal{O}(x^4)$, while the non-analytic one is absent. It is important to note that even though b_3 (6) can be omitted at $T > T_A$, \mathcal{C} also enters into the c_2 coefficient (5), and still plays a role until very high temperatures are reached, where $g_1(x)_{\text{MB}}$ is valid.

Momentum Distribution.— The momentum distribution is related to the OBDM (3) by a Fourier transform (FT) [8]

$$n(k) = \frac{1}{n} \int_{-\infty}^{+\infty} \frac{dx}{2\pi\hbar} \cos(k \cdot x) g_1(x), \quad (8)$$

and gives the probability to find an atom with momentum k .

In a 1D Bose gas, $n(k)$ has been calculated numerically at $T = 0$ with the diffusion Monte Carlo technique [54, 55].

At finite temperature, the weakly-interacting limit at low temperature has been studied with the analytical Bogoliubov approach [56], while for strong interactions with PIMC [26] and the numerical stochastic gauge technique for just one value of temperature [57]. At temperature below the hole anomaly, $n(k)$ has been computed with the form factor approach [58].

Our work fills an important gap: we compute $n(k)$ in a 1D Bose gas with the PIMC method, exploring all regimes from weak to strong interactions and from low to high temperatures [53]. To this aim, we apply the FT (8) to the PIMC results for the OBDM [49]. At high T , the momentum distribution approaches the Gaussian shape, $n(k)_{\text{MB}} = \sigma / (\hbar\sqrt{2\pi}) e^{-\sigma^2 k^2/2}$ typical of a classical gas [53].

We derive the large- k tail of $n(k)$ by using the short-distance OBDM (4) in Eq. (8), where we integrate up to $x_{\max} = k_{\min}^{-1}$ (7) fixing the minimum momentum for the tail:

$$n(|k| \gtrsim k_{\min}) = \frac{6n^3 b_3}{\pi\hbar k^4} \left[1 - \cos\left(\frac{k}{k_{\min}}\right) \right] - \frac{1}{\pi\hbar|k|^3} \sin\left(\frac{|k|}{k_{\min}}\right) \left(2c_2 n^2 + \frac{6n^3 b_3}{k_{\min}} \right) + \mathcal{O}\left(\frac{1}{k^2}\right). \quad (9)$$

The $1/k^4$ term emerges from the leading non-analytic behavior of the short-distance OBDM whose coefficient is b_3 (6) and provides the universal tail \mathcal{C}/k^4 derived for the 1D Bose gas at $T = 0$ [9]. The $1/|k|^3$ -term depends also on the c_2 coefficient which is a function of the internal energy and contact, Eq. (5), as well as the momentum k_{\min} .

In Fig. 3, we show the PIMC results for the momentum distribution $n(k)$, similarly to Fig. 2. The interacting regimes with $\gamma = 10^{-1}$ (first and second panels) and $\gamma = 1$ (last) are reported. The main panel shows the complete k -dependence. In the insets, we compare the large- k tail (9) with $b_3 \neq 0$ (colored solid lines) and $b_3 = 0$ (black dashed), calculated with TBA. $k_{\min} = x_{\max}^{-1}$ (7) is shown with vertical lines.

At $T = 0$, the occupation of the zero-momentum state features a power-law divergence with the particle number

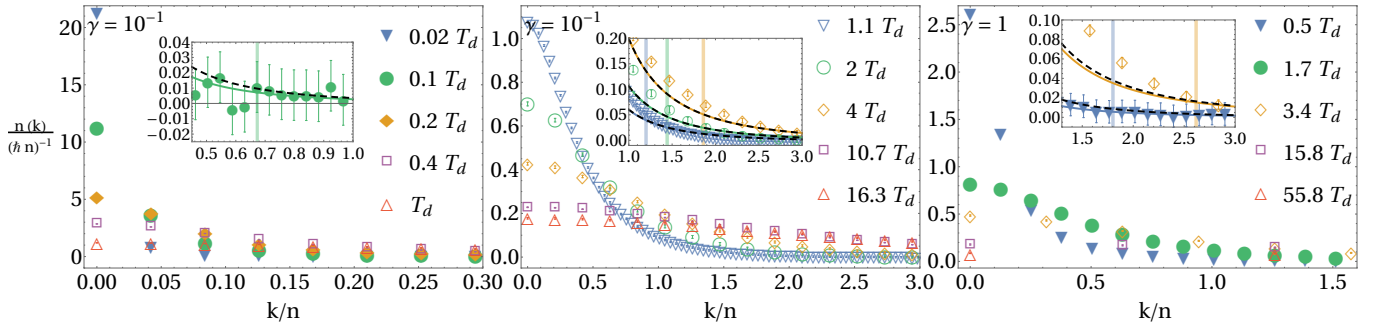


Figure 3. Momentum distribution $n(k)$ for $\gamma = 10^{-1}$ (first and second panels) and $\gamma = 1$ (last) and different temperatures. Solid (empty) symbols correspond to $T < T_A$ ($T > T_A$) and show PIMC results. In the insets, solid (dashed black) lines represent the large- k behavior (9) with $b_3 \neq 0$ ($b_3 = 0$), calculated with TBA and reported in increasing order of the temperature from low (bottom) to high (top) values. $k_{\min}/n = (x_{\max}n)^{-1}$ (vertical lines) is reported with increasing order of temperature from low (left) to high (right) values in each inset.

$n(k=0) \propto N^{1-1/(2K)}$ where $K \geq 1$ is the Luttinger parameter [52]. This is a remnant of the Bose-Einstein condensation, which is reached only asymptotically in the weakly-interacting limit, $\gamma \rightarrow 0$ ($K \rightarrow \infty$), where $n(k=0) \propto N$. At finite temperature, the peak in $n(k=0)$ is smeared and the divergence is removed, see Fig. 3. It gets smaller and broader with the increase of T and γ [53]. For $\gamma = 10^{-1}$ and low temperatures, the peak is high, consistently with the presence of a quasicondensate [59], but it does not show a delta-function behavior typical of a true condensate in higher spatial dimensions. The thermal disappearance of the quasicondensate has been also found in other correlation properties [49].

In Fig. 4, we report $n(k)k^4$ for $\gamma = 10^{-1}$ to check the thermal fading in the distribution tail at high temperatures. Horizontal lines denote the universal tail $6n^3b_3/(\pi\hbar)$ of Eq. (9).

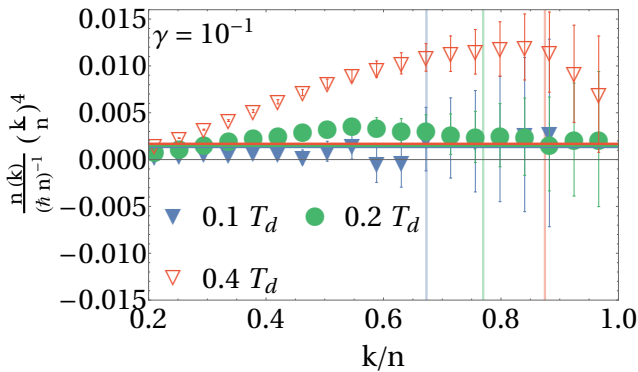


Figure 4. $n(k)k^4$ vs momentum k for $\gamma = 10^{-1}$. Solid (empty) symbols correspond to temperatures below (above) the anomaly T_A and represent PIMC results. $k_{\min}/n = (x_{\max}n)^{-1}$ is denoted by vertical lines with increasing temperature from low (left) to high (right) values. Horizontal lines report the tail $6n^3b_3/(\pi\hbar)$ of Eq. (9) calculated with TBA and they overlap at different temperatures.

Consistently with the short-distance OBDM of Fig. 2, from Figs. 3 and 4, we get the general results, for any interaction strength γ , for the momentum distribution: (i) the complete large- k tail (9) and its range limit k_{\min} hold at any temperature, as shown by comparison with PIMC; (ii) the universal

tail $b_3/k^4 \sim \mathcal{C}/k^4$ is valid only for temperatures smaller than the anomaly threshold $T < T_A$, while at $T > T_A$ becomes negligible. The deviation from the \mathcal{C}/k^4 -tail in Fig. 4 is more evident by further increasing the temperature [53].

Experimental Considerations.— 1D atomic Bose gases can be realized with a single optical tube trap [31] which allows for the exploration of temperature below and above the hole anomaly. Spatial uniform density is achieved with a flatbox potential [60]. The interaction strength $\gamma \sim 1/(na)$ is tuned by changing the density n via the strongly confining potential in the radial directions [32, 35, 37] or by adjusting the scattering length a through Fano-Feshbach resonances [29, 61]. Temperature can be extracted from a single absorption image during time-of-flight (TOF) expansion with neural network [62]. In a 1D Bose gas, $n(k)$ is measured with Bragg spectroscopy [27, 63], Bose-gas focusing [28] and TOF expansion combined with absorption image [64], without [29, 34, 65, 66] and with focusing technique [30].

Conclusions.— We analytically and numerically study the momentum distribution and the one-body density matrix in a 1D repulsive Bose gas, in all contact-interaction and temperature regimes. We employ Bethe-Ansatz and Path Integral Monte Carlo methods whose results serve as a universal benchmark for our theories and experiments. For any interaction strength, we find that: (i) the hole anomaly induces a thermal increase of the internal energy which is responsible for the high-temperature fadings of the large- k tail \mathcal{C}/k^4 in the momentum distribution $n(k)$ and the $|x|^3$ -dependence of the OBDM at short distances; (ii) we establish the limits of the validity range for large-momenta and short-distance properties and they hold at arbitrary temperature; (iii) we derive a general tail for $n(k)$ (9) containing the $1/|k|^3$ term, which becomes dominant for temperatures above the anomaly ($T > T_A$).

Perspectives include the harmonically-trapped configuration [26, 67–71] where the $n(k)$ -tail has been studied at $T < T_A$ [47]. Breathing-mode frequencies [72–74] are sensitive to the regime [75] and at high temperature, the two-frequency excitation identifies the collisionless regime [76]. This T -induced hydrodynamic-collisionless transition [76] may be an

effect of the hole anomaly [20]. Our findings can be extended to the super Tonks-Girardeau gas [77, 78], dipolar Bose gases [79], ^4He liquids [80], liquids in bosonic mixtures [81], lattices [82] and spin-orbital coupling settings [83]. Other violations of the law $n(k) \sim C/k^4$ have been found in the presence of particle losses [84], interactions with impurities [85] and hard-wall boundaries [86].

G. D. R.'s received funding from the grant IJC2020-043542-I funded by MCIN/AEI/10.13039/501100011033 and by "European Union NextGenerationEU/PRTR". G. D. R., G. E. A. and J. B. were partially supported by grant PID2020-113565GB-C21 funded by MCIN/AEI/10.13039/501100011033. M.O was supported by the NSF grant PHY-1912542.

* giulia.de.rosi@upc.edu

† grigori.astrakharchik@upc.edu

‡ jordi.boronat@upc.edu

[1] L. N. Cooper, *Bound Electron Pairs in a Degenerate Fermi Gas*, *Phys. Rev.* **104**, 1189 (1956).

[2] J. Bardeen, L. N. Cooper, and J. R. Schrieffer, *Microscopic Theory of Superconductivity*, *Phys. Rev.* **106**, 162 (1957).

[3] J. Bardeen, L. N. Cooper, and J. R. Schrieffer, *Theory of Superconductivity*, *Phys. Rev.* **108**, 1175 (1957).

[4] S. Giorgini, L. P. Pitaevskii, and S. Stringari, *Theory of ultracold atomic Fermi gases*, *Rev. Mod. Phys.* **80**, 1215 (2008).

[5] M. H. Anderson, J. R. Ensher, M. R. Matthews, C. E. Wieman, and E. A. Cornell, *Observation of Bose-Einstein Condensation in a Dilute Atomic Vapor*, *Science* **269**, 198 (1995).

[6] K. B. Davis, M. O. Mewes, M. R. Andrews, N. J. van Druten, D. S. Durfee, D. M. Kurn, and W. Ketterle, *Bose-Einstein Condensation in a Gas of Sodium Atoms*, *Phys. Rev. Lett.* **75**, 3969 (1995).

[7] F. Dalfovo, S. Giorgini, L. P. Pitaevskii, and S. Stringari, *Theory of Bose-Einstein condensation in trapped gases*, *Rev. Mod. Phys.* **71**, 463 (1999).

[8] L. Pitaevskii and S. Stringari, *Bose-Einstein Condensation and Superfluidity*, International Series of Monographs on Physics (Oxford University Press, Oxford, 2016).

[9] M. Olshanii and V. Dunjko, *Short-Distance Correlation Properties of the Lieb-Liniger System and Momentum Distributions of Trapped One-Dimensional Atomic Gases*, *Phys. Rev. Lett.* **91**, 090401 (2003).

[10] S. Tan, *Energetics of a strongly correlated Fermi gas*, *Annals of Physics* **323**, 2952 (2008).

[11] S. Tan, *Generalized virial theorem and pressure relation for a strongly correlated Fermi gas*, *Annals of Physics* **323**, 2987 (2008).

[12] S. Tan, *Large momentum part of a strongly correlated Fermi gas*, *Annals of Physics* **323**, 2971 (2008).

[13] A. Bulgac, *Entropy, single-particle occupation probabilities, and short-range correlations*, *arXiv:2203.12079* (2022).

[14] M. Barth and W. Zwerger, *Tan relations in one dimension*, *Annals of Physics* **326**, 2544 (2011).

[15] N. Matveeva and G. E. Astrakharchik, *One-dimensional multi-component Fermi gas in a trap: quantum Monte Carlo study*, *New Journal of Physics* **18**, 065009 (2016).

[16] O. I. Pătu and A. Klümper, *Universal Tan relations for quantum gases in one dimension*, *Phys. Rev. A* **96**, 063612 (2017).

[17] J. E. Drut, T. A. Lähde, and T. Ten, *Momentum Distribution and Contact of the Unitary Fermi Gas*, *Phys. Rev. Lett.* **106**, 205302 (2011).

[18] J. T. Stewart, J. P. Gaebler, T. E. Drake, and D. S. Jin, *Verification of Universal Relations in a Strongly Interacting Fermi Gas*, *Phys. Rev. Lett.* **104**, 235301 (2010).

[19] P. Makotyn, C. E. Klauss, D. L. Goldberger, E. A. Cornell, and D. S. Jin, *Universal dynamics of a degenerate unitary Bose gas*, *Nature Physics* **10**, 116 (2014).

[20] G. De Rosi, R. Rota, G. E. Astrakharchik, and J. Boronat, *Hole-induced anomaly in the thermodynamic behavior of a one-dimensional Bose gas*, *SciPost Phys.* **13**, 035 (2022).

[21] D. C. Dender, P. R. Hammar, D. H. Reich, C. Broholm, and G. Aeppli, *Direct Observation of Field-Induced Incommensurate Fluctuations in a One-Dimensional $S = 1/2$ Antiferromagnet*, *Phys. Rev. Lett.* **79**, 1750 (1997).

[22] P. R. Hammar, M. B. Stone, D. H. Reich, C. Broholm, P. J. Gibson, M. M. Turnbull, C. P. Landee, and M. Oshikawa, *Characterization of a quasi-one-dimensional spin-1/2 magnet which is gapless and paramagnetic for $g\mu_B H \lesssim J$ and $k_B T \ll J$* , *Phys. Rev. B* **59**, 1008 (1999).

[23] C. Rüegg, K. Kiefer, B. Thielemann, D. F. McMorrow, V. Zapf, B. Normand, M. B. Zvonarev, P. Bouillot, C. Kollath, T. Giarmachi, S. Capponi, D. Poilblanc, D. Biner, and K. W. Krämer, *Thermodynamics of the Spin Luttinger Liquid in a Model Ladder Material*, *Phys. Rev. Lett.* **101**, 247202 (2008).

[24] P. Bouillot, C. Kollath, A. M. Läuchli, M. Zvonarev, B. Thielemann, C. Rüegg, E. Orignac, R. Citro, M. Klanjšek, C. Berthier, M. Horvatić, and T. Giarmachi, *Statics and dynamics of weakly coupled antiferromagnetic spin- $\frac{1}{2}$ ladders in a magnetic field*, *Phys. Rev. B* **83**, 054407 (2011).

[25] L. D. Landau and E. M. Lifshitz, *Statistical Physics: Vol. 5* (Elsevier Science, 2013).

[26] W. Xu and M. Rigol, *Universal scaling of density and momentum distributions in Lieb-Liniger gases*, *Phys. Rev. A* **92**, 063623 (2015).

[27] S. Richard, F. Gerbier, J. H. Thywissen, M. Hugbart, P. Bouyer, and A. Aspect, *Momentum Spectroscopy of 1D Phase Fluctuations in Bose-Einstein Condensates*, *Phys. Rev. Lett.* **91**, 010405 (2003).

[28] A. H. van Amerongen, J. J. P. van Es, P. Wicke, K. V. Kheruntsyan, and N. J. van Druten, *Yang-Yang Thermodynamics on an Atom Chip*, *Phys. Rev. Lett.* **100**, 090402 (2008).

[29] F. Meinert, M. Panfil, M. J. Mark, K. Lauber, J.-S. Caux, and H.-C. Nägerl, *Probing the Excitations of a Lieb-Liniger Gas from Weak to Strong Coupling*, *Phys. Rev. Lett.* **115**, 085301 (2015).

[30] B. Yang, Y.-Y. Chen, Y.-G. Zheng, H. Sun, H.-N. Dai, X.-W. Guan, Z.-S. Yuan, and J.-W. Pan, *Quantum criticality and the Tomonaga-Luttinger liquid in one-dimensional Bose gases*, *Phys. Rev. Lett.* **119**, 165701 (2017).

[31] F. Salces-Carcoba, C. J. Billington, A. Putra, Y. Yue, S. Sugawa, and I. B. Spielman, *Equations of state from individual one-dimensional Bose gases*, *New Journal of Physics* **20**, 113032 (2018).

[32] M. Olshanii, *Atomic Scattering in the Presence of an External Confinement and a Gas of Impenetrable Bosons*, *Phys. Rev. Lett.* **81**, 938 (1998).

[33] M. Girardeau, *Relationship between Systems of Impenetrable Bosons and Fermions in One Dimension*, *Journal of Mathematical Physics* **1**, 516 (1960).

[34] B. Paredes, A. Widera, V. Murg, O. Mandel, S. Fölling, I. Cirac, G. V. Shlyapnikov, T. W. Hänsch, and I. Bloch, *Tonks-*

Girardeau gas of ultracold atoms in an optical lattice, *Nature* **429**, 277 EP (2004).

[35] T. Kinoshita, T. Wenger, and D. S. Weiss, *Observation of a One-Dimensional Tonks-Girardeau Gas*, *Science* **305**, 1125 (2004).

[36] B. Laburthe Tolra, K. M. O'Hara, J. H. Huckans, W. D. Phillips, S. L. Rolston, and J. V. Porto, *Observation of Reduced Three-Body Recombination in a Correlated 1D Degenerate Bose Gas*, *Phys. Rev. Lett.* **92**, 190401 (2004).

[37] T. Kinoshita, T. Wenger, and D. S. Weiss, *Local Pair Correlations in One-Dimensional Bose Gases*, *Phys. Rev. Lett.* **95**, 190406 (2005).

[38] E. Haller, M. Rabie, M. J. Mark, J. G. Danzl, R. Hart, K. Lauber, G. Pupillo, and H.-C. Nägerl, *Three-Body Correlation Functions and Recombination Rates for Bosons in Three Dimensions and One Dimension*, *Phys. Rev. Lett.* **107**, 230404 (2011).

[39] T. Jacqmin, J. Armijo, T. Berrada, K. V. Kheruntsyan, and I. Bouchoule, *Sub-Poissonian Fluctuations in a 1D Bose Gas: From the Quantum Quasicondensate to the Strongly Interacting Regime*, *Phys. Rev. Lett.* **106**, 230405 (2011).

[40] V. Guarnera, D. Muth, R. Labouvie, A. Vogler, G. Barontini, M. Fleischhauer, and H. Ott, *Spatiotemporal fermionization of strongly interacting one-dimensional bosons*, *Phys. Rev. A* **86**, 021601(R) (2012).

[41] E. H. Lieb and W. Liniger, *Exact Analysis of an Interacting Bose Gas. I. The General Solution and the Ground State*, *Phys. Rev.* **130**, 1605 (1963).

[42] E. H. Lieb, *Exact Analysis of an Interacting Bose Gas. II. The Excitation Spectrum*, *Phys. Rev.* **130**, 1616 (1963).

[43] G. De Rosi, G. E. Astrakharchik, and S. Stringari, *Thermodynamic behavior of a one-dimensional Bose gas at low temperature*, *Phys. Rev. A* **96**, 013613 (2017).

[44] C. N. Yang and C. P. Yang, *Thermodynamics of a One-Dimensional System of Bosons with Repulsive Delta-Function Interaction*, *Journal of Mathematical Physics* **10**, 1115 (1969).

[45] C. P. Yang, *One-Dimensional System of Bosons with Repulsive δ -Function Interactions at a Finite Temperature T* , *Phys. Rev. A* **2**, 154 (1970).

[46] E. Braaten, D. Kang, and L. Platter, *Universal Relations for Identical Bosons from Three-Body Physics*, *Phys. Rev. Lett.* **106**, 153005 (2011).

[47] H. Yao, D. Clément, A. Minguzzi, P. Vignolo, and L. Sanchez-Palencia, *Tan's Contact for Trapped Lieb-Liniger Bosons at Finite Temperature*, *Phys. Rev. Lett.* **121**, 220402 (2018).

[48] G. De Rosi, P. Massignan, M. Lewenstein, and G. E. Astrakharchik, *Beyond-Luttinger-liquid thermodynamics of a one-dimensional Bose gas with repulsive contact interactions*, *Phys. Rev. Research* **1**, 033083 (2019).

[49] G. De Rosi, R. Rota, G. E. Astrakharchik, and J. Boronat, *Correlation properties of a one-dimensional repulsive Bose gas at finite temperature*, *arXiv:2301.07626* (2023).

[50] G. E. Astrakharchik, D. M. Gangardt, Y. E. Lozovik, and I. A. Sorokin, *Off-diagonal correlations of the Calogero-Sutherland model*, *Phys. Rev. E* **74**, 021105 (2006).

[51] R. P. Feynman, *Forces in Molecules*, *Phys. Rev.* **56**, 340 (1939).

[52] M. A. Cazalilla, *Bosonizing one-dimensional cold atomic gases*, *Journal of Physics B: Atomic, Molecular and Optical Physics* **37**, S1 (2004).

[53] See Supplemental Material at [...] for additional results for the OBDM and the momentum distribution, including the Maxwell-Boltzmann regime of the classical gas at high temperatures. The Supplemental Material includes Ref. [49].

[54] G. E. Astrakharchik and S. Giorgini, *Correlation functions and momentum distribution of one-dimensional Bose systems*, *Phys. Rev. A* **68**, 031602(R) (2003).

[55] G. E. Astrakharchik and S. Giorgini, *Correlation functions of a Lieb-Liniger Bose gas*, *Journal of Physics B: Atomic, Molecular and Optical Physics* **39**, S1 (2006).

[56] C. Mora and Y. Castin, *Extension of Bogoliubov theory to quasi-condensates*, *Phys. Rev. A* **67**, 053615 (2003).

[57] P. D. Drummond, P. Deuar, and K. V. Kheruntsyan, *Canonical Bose Gas Simulations with Stochastic Gauges*, *Phys. Rev. Lett.* **92**, 040405 (2004).

[58] S. Cheng, Y.-Y. Chen, X.-W. Guan, W.-L. Yang, and H.-Q. Lin, *One-body dynamical correlation function of Lieb-Liniger model at finite temperature*, *arXiv:2211.00282* (2022).

[59] J. Esteve, J.-B. Trebbia, T. Schumm, A. Aspect, C. I. Westbrook, and I. Bouchoule, *Observations of Density Fluctuations in an Elongated Bose Gas: Ideal Gas and Quasicondensate Regimes*, *Phys. Rev. Lett.* **96**, 130403 (2006).

[60] B. Rauer, S. Erne, T. Schweigler, F. Cataldini, M. Tajik, and J. Schmiedmayer, *Recurrences in an isolated quantum many-body system*, *Science* **360**, 307 (2018).

[61] C. Chin, R. Grimm, P. Julienne, and E. Tiesinga, *Feshbach resonances in ultracold gases*, *Rev. Mod. Phys.* **82**, 1225 (2010).

[62] F. Møller, T. Schweigler, M. Tajik, J. a. Sabino, F. Cataldini, S.-C. Ji, and J. Schmiedmayer, *Thermometry of one-dimensional Bose gases with neural networks*, *Phys. Rev. A* **104**, 043305 (2021).

[63] N. Fabbri, D. Clément, L. Fallani, C. Fort, and M. Inguscio, *Momentum-resolved study of an array of one-dimensional strongly phase-fluctuating Bose gases*, *Phys. Rev. A* **83**, 031604 (2011).

[64] Y. Le, Y. Zhang, S. Gopalakrishnan, M. Rigol, and D. S. Weiss, *Direct observation of hydrodynamization and local prethermalization*, *arXiv:2210.07318* (2022).

[65] J. M. Wilson, N. Malvania, Y. Le, Y. Zhang, M. Rigol, and D. S. Weiss, *Observation of dynamical fermionization*, *Science* **367**, 1461 (2020).

[66] N. Malvania, Y. Zhang, Y. Le, J. Dubail, M. Rigol, and D. S. Weiss, *Generalized hydrodynamics in strongly interacting 1D Bose gases*, *Science* **373**, 1129 (2021).

[67] D. S. Petrov, G. V. Shlyapnikov, and J. T. M. Walraven, *Regimes of Quantum Degeneracy in Trapped 1D Gases*, *Phys. Rev. Lett.* **85**, 3745 (2000).

[68] K. V. Kheruntsyan, D. M. Gangardt, P. D. Drummond, and G. V. Shlyapnikov, *Finite-temperature correlations and density profiles of an inhomogeneous interacting one-dimensional Bose gas*, *Phys. Rev. A* **71**, 053615 (2005).

[69] M. J. Davis, P. B. Blakie, A. H. van Amerongen, N. J. van Druten, and K. V. Kheruntsyan, *Yang-Yang thermometry and momentum distribution of a trapped one-dimensional Bose gas*, *Phys. Rev. A* **85**, 031604 (2012).

[70] P. Vignolo and A. Minguzzi, *Universal Contact for a Tonks-Girardeau Gas at Finite Temperature*, *Phys. Rev. Lett.* **110**, 020403 (2013).

[71] A. Minguzzi and P. Vignolo, *Strongly interacting trapped one-dimensional quantum gases: an exact solution*, *arXiv:2201.02362* (2022).

[72] H. Moritz, T. Stöferle, M. Köhl, and T. Esslinger, *Exciting Collective Oscillations in a Trapped 1D Gas*, *Phys. Rev. Lett.* **91**, 250402 (2003).

[73] H. Hu, G. Xianlong, and X.-J. Liu, *Collective modes of a one-dimensional trapped atomic Bose gas at finite temperatures*, *Phys. Rev. A* **90**, 013622 (2014).

[74] B. Fang, G. Carleo, A. Johnson, and I. Bouchoule, *Quench-Induced Breathing Mode of One-Dimensional Bose Gases*, *Phys. Rev. Lett.* **113**, 035301 (2014).

[75] G. De Rosi and S. Stringari, *Collective oscillations of a trapped quantum gas in low dimensions*, *Phys. Rev. A* **92**, 053617 (2015).

[76] G. De Rosi and S. Stringari, *Hydrodynamic versus collisionless dynamics of a one-dimensional harmonically trapped Bose gas*, *Phys. Rev. A* **94**, 063605 (2016).

[77] G. E. Astrakharchik, J. Boronat, J. Casulleras, and S. Giorgini, *Beyond the Tonks-Girardeau Gas: Strongly Correlated Regime in Quasi-One-Dimensional Bose Gases*, *Phys. Rev. Lett.* **95**, 190407 (2005).

[78] E. Haller, M. Gustavsson, M. J. Mark, J. G. Danzl, R. Hart, G. Pupillo, and H.-C. Nägerl, *Realization of an Excited, Strongly Correlated Quantum Gas Phase*, *Science* **325**, 1224 (2009).

[79] K.-Y. Li, Y. Zhang, K. Yang, K.-Y. Lin, S. Gopalakrishnan, M. Rigol, and B. L. Lev, *Rapidity and momentum distributions of 1D dipolar quantum gases*, *arXiv:2211.09118* (2022).

[80] A. Del Maestro, N. Nichols, T. Prisk, G. Warren, and P. E. Sokol, *Experimental realization of one dimensional helium*, *Nature Comm.* **13**, 3168 (2022).

[81] G. De Rosi, G. E. Astrakharchik, and P. Massignan, *Thermal instability, evaporation, and thermodynamics of one-dimensional liquids in weakly interacting Bose-Bose mixtures*, *Phys. Rev. A* **103**, 043316 (2021).

[82] M. Rigol, *Finite-temperature properties of hard-core bosons confined on one-dimensional optical lattices*, *Phys. Rev. A* **72**, 063607 (2005).

[83] F. Qin and P. Zhang, *Universal relations for hybridized s - and p -wave interactions from spin-orbital coupling*, *Phys. Rev. A* **102**, 043321 (2020).

[84] I. Bouchoule and J. Dubail, *Breakdown of Tan's Relation in Lossy One-Dimensional Bose Gases*, *Phys. Rev. Lett.* **126**, 160603 (2021).

[85] H. Cayla, P. Massignan, T. Giamarchi, A. Aspect, C. I. Westbrook, and D. Clément, *Observation of $1/k^4$ -tails in the asymptotic momentum distribution of Bose polarons*, *arXiv:2204.10697* (2022).

[86] G. Aupetit-Diallo, S. Musolino, M. Albert, and P. Vignolo, *High-momentum oscillating tails of strongly interacting 1D gases in a box*, *arXiv:2302.02828* (2023).

Supplemental Material for “Thermal fading of the $1/k^4$ -tail of the momentum distribution induced by the hole anomaly”

Giulia De Rosi,^{1,*} Grigori E. Astrakharchik,^{1,2,†} Maxim Olshanii,³ and Jordi Boronat^{1,‡}

¹Departament de Física, Universitat Politècnica de Catalunya, Campus Nord B4-B5, 08034 Barcelona, Spain

²Departament de Física Quàntica i Astrofísica, Facultat de Física, Universitat de Barcelona, E-08028 Barcelona, Spain

³Department of Physics, University of Massachusetts Boston, Boston Massachusetts 02125, USA

(Dated: February 13, 2023)

In this Supplemental Material, we provide additional results for the one-body density matrix (Sec. S1) and the momentum distribution (Sec. S2). Several characteristic values of the interaction strength γ and temperatures smaller and larger than the hole-anomaly threshold T_A (see Fig. 1 in the main text) have been considered. Our findings also include the Maxwell-Boltzmann (MB) regime corresponding to the classical gas at very high temperatures.

S1. ONE-BODY DENSITY MATRIX

In Fig. S1, we report with symbols the exact Path Integral Monte Carlo (PIMC) results for the one-body density matrix (OBDM) $g_1(x)$ for temperatures $T > T_A$ in units of the quantum degeneracy value $T_d = \hbar^2 n^2 / (2m k_B)$. The weakly- [$\gamma = 10^{-1}$, panels a)-b)], intermediate- [$\gamma = 1$, c)] and strongly- [$\gamma = 10$, d)] interacting regimes are shown. In panel a), we consider the intermediate temperature regime, while in b)-d) the MB classical gas. We compare the short-distance expansion of the OBDM (Eq. (4) of the main text) with (without) the cubic term (whose coefficient is b_3) reported with coloured solid (black dashed) lines and calculated with thermal Bethe-Ansatz (TBA) method. The maximal distance $x_{\max} = (\xi^{-1} + \sigma^{-1})^{-1}$ (also defined in Eq. (7) in the main text) for the validity of the short-distance behavior is represented with vertical lines.

PIMC results in panels b)-d) show an excellent agreement with the analytical MB limit $g_1(x)_{\text{MB}}$ [1] reported in the main text.

Our findings for x_{\max} and the thermal fading of the cubic spatial dependence of the short-distance OBDM for temperature values larger than the anomaly reference are also valid in the regimes of Fig. S1, as witnessed by comparison with PIMC results.

S2. MOMENTUM DISTRIBUTION

In Fig. S2, we report with symbols the PIMC results of the momentum distribution $n(k)$. In panels a), c) and f) we consider the MB regime; in b) very low temperature below the hole anomaly $T < T_A$; in d) around the hole anomaly and in e) the virial hard-core regime [1]. Dashed lines in the MB panels denote the analytical MB limit $n(k)_{\text{MB}}$ reported in the main text and which exhibits an agreement with PIMC findings for any interaction strength γ . We observe a peak at small momentum k which gets smaller and broader with the increase of temperature and γ .

In Fig. S3, we report $n(k)k^4$ for $\gamma = 10^{-1}$ and temperature above the anomaly $T > T_A$. We show the minimum momentum $k_{\min} = x_{\max}^{-1}$ for the large- k behavior with vertical lines. Horizontal lines report the universal large- k tail $6n^3 b_3 / (\pi \hbar) \sim \mathcal{C}$ computed with TBA and where \mathcal{C} is the Tan’s contact. As discussed in the main text, the coefficient of this large-momentum behavior becomes negligible $b_3 \approx 0$ at $T > T_A$, by inducing the deviation from the universal tail at high temperatures.

* giulia.de.rosi@upc.edu

† grigori.astrakharchik@upc.edu

‡ jordi.boronat@upc.edu

[1] G. De Rosi, R. Rota, G. E. Astrakharchik, and J. Boronat, *Correlation properties of a one-dimensional repulsive Bose gas at finite temperature*, [arXiv:2301.07626](https://arxiv.org/abs/2301.07626) (2023).

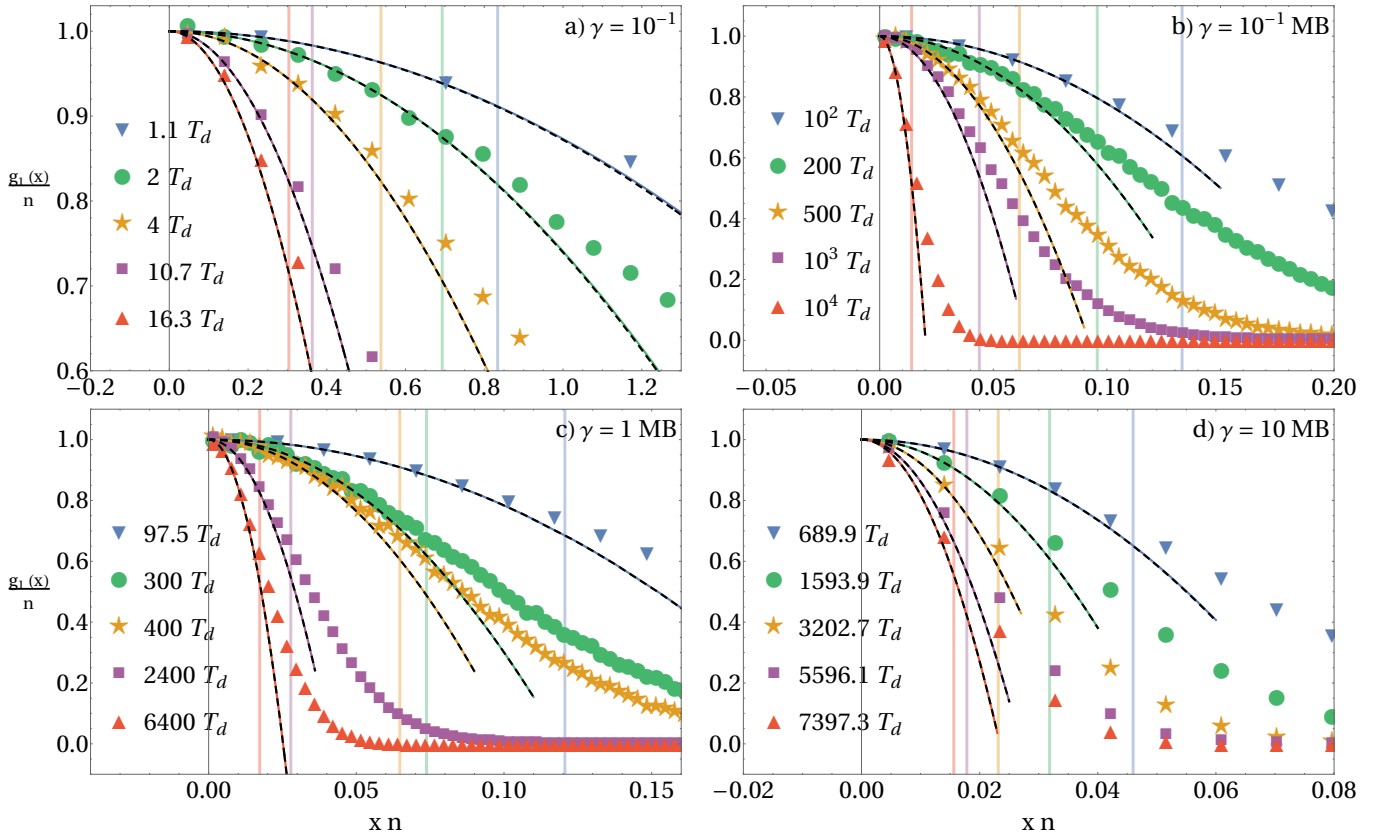


Figure S1. OBDM $g_1(x)/n$ vs relative distance x in units of the inverse density n^{-1} for a) $\gamma = 10^{-1}$ at the intermediate temperature regime; b-d) MB regime for $\gamma = 10^{-1}, 1$, and 10 , respectively. Different values of temperature in units of the quantum degeneracy value $T_d = \hbar^2 n^2 / (2m k_B)$ are reported. Symbols denote PIMC results and their sizes are larger than the error bars. Solid lines represent the complete expansion at short distances calculated with TBA. Dashed black lines correspond to the same, but without the cubic term. All curves are reported in increasing order of the temperature from low (top) to high (bottom) values. $x_{\max} n = (\xi^{-1} + \sigma^{-1})^{-1} n$ is represented by vertical lines with increasing order of temperature from low (right) to high (left) values in each panel.

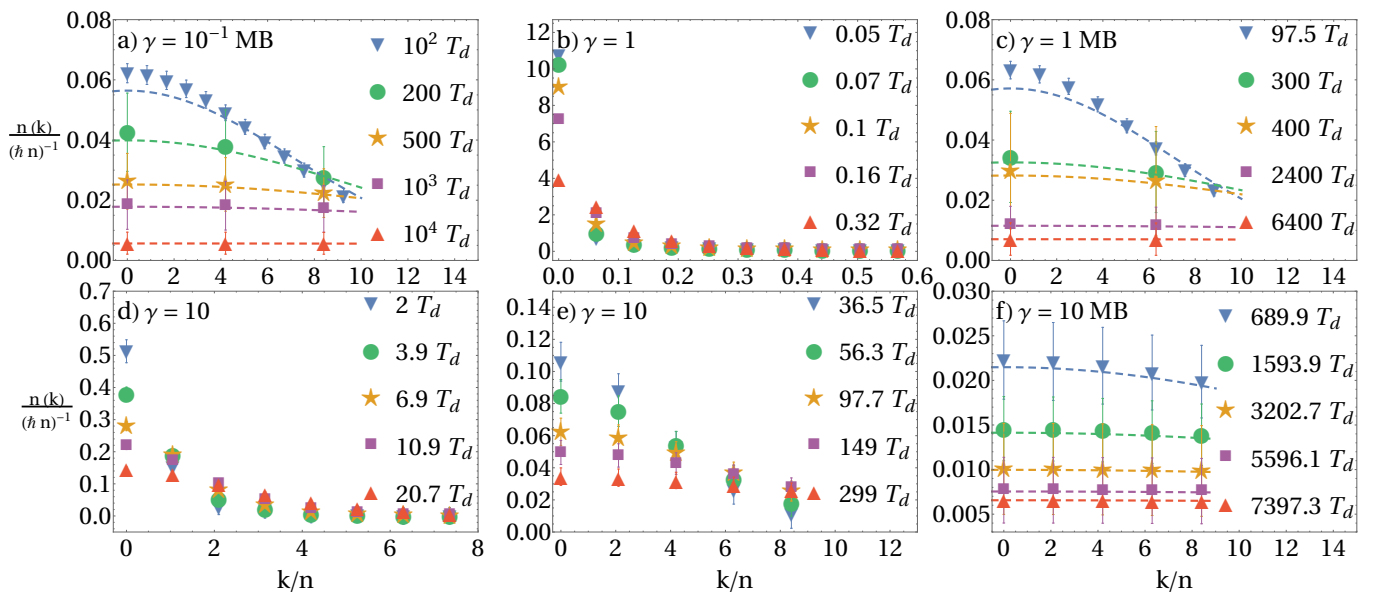


Figure S2. Momentum distribution $n(k)$ for a) $\gamma = 10^{-1}$ in the MB regime; b) $\gamma = 1$ at $T < T_A$; c) $\gamma = 1$ in the MB limit; d-f) $\gamma = 10$ around the hole anomaly, virial hard-core and MB regime, respectively. Symbols denote PIMC results. Dashed lines correspond to the MB limit $n(k)_{\text{MB}}$ and are shown in increasing order of the temperature from low (top) to high (bottom) values in each MB panel.

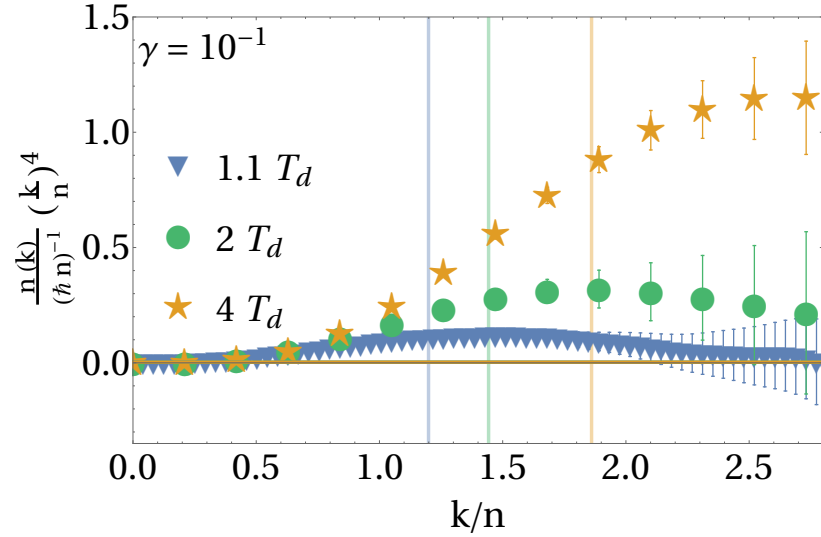


Figure S3. $n(k)k^4$ vs momentum k for $\gamma = 10^{-1}$. Symbols correspond to PIMC results. $k_{\min}/n = (x_{\max}n)^{-1}$ is represented by vertical lines with increasing order of temperature from low (left) to high (right) values. Horizontal lines report the tail $6n^3 b_3 / (\pi \hbar)$ calculated with TBA and overlapping at different temperatures.